Iranica Journal of Energy & Environment
Journal Homepage: www.ijee.net
IJEE an official peer review journal of Babol Noshirvani University of Technology, ISSN:2079-2115

Energy and Exergy Study of a Nanofluid-based Solar System Integrated with a Quadruple Effect Absorption Cycle and Thermoelectric Generator

M. Mahmoudi, I. Mirzaee*, M. Khalilian

Mechanical Engineering Department, Faculty of Engineering, Urmia University, Urmia, Iran

P A P E R I N F O

Paper history:
Received 13 May 2023
Accepted in revised form 13 July 2023

Keywords:
Multigeneration system
Nanofluids
Solar collector
The quadruple effect absorption cycle
Thermoelectric generator

A B S T R A C T

The exploitation of nanofluids is the most noteworthy way to make better the rate of heat transfer in solar collectors. Moreover, recently utilizing thermoelectric generators are widely studied to direct the conversion of heat into electricity. The objective of the present study is to deal with a novel multigeneration system that includes a nanofluid-based parabolic trough collector integrated with a quadruple effect absorption refrigeration cycle (cooling), a thermoelectric generator (power), a PEM electrolyzer (hydrogen), vapor generator and domestic water heater. A parametric study is accomplished to consider the effect of significant parameters such as the volume concentration of nanoparticles, solar radiation, absorption system's generator load, strong solution concentration, and TEG's figure of merit on the overall system performance, hydrogen production rate, cooling load, COP and useful energy obtained by the collector. It is observed that the power generated by the system is 18.78 kW and the collector energy and exergy efficiency are 82.21% and 80.48%, respectively. Furthermore, the results showed that the highest exergy destruction rate occurs in the solar system at the rate of 4461 kW. The energy and exergy COPs of the absorption chiller are discovered to be 1.527 and 0.936, respectively. By increasing the concentration of nanoparticles and the amount of solar radiation, the amount of collector useful energy increases while the hydrogen production rate and the generated power in the TEG decreased. The cooling capacity and COPs of the absorption system increased with an increase in VHTG load and decreased with an increase in concentration of the strong solution.

***doi**: 10.5829/ijee.2024.15.01.08*

NOMENCLATURE

A	Area (m^2)	ZT_m	Figure of merit
C_p	Specific heat capacity (J/kgK)	**Subscripts**	
D	Collector diameter (m)	0	Ambient
E	Energy input (kW)	1,2,…	State points
$\dot{E}x$	Exergy rate (W)	abs	Absorber
ex	Exergy (J/kg)	ap	Aperture
F_1	Collector efficiency factor	ARS	Absorption refrigeration cycle
F_R	Heat transfer factor	bf	Base fluid
G	Solar irradiation (W/m^2)	con	Condenser
h	Entalphy	COP	Coefficient of performance
J	Current density (A/m^2)	D	Destroyed
k	Thermal conductivity (W/m K)	DWH	Domestic water heater
L	Collector length (m)	e	Out
M	Molecular weight (kg/mol)	eva	Evaporator

* Corresponding Author Email: i.mirzaee@urmia.ac.ir (I. Mirzaee)

Please cite this article as: M. Mahmoudi, I. Mirzaee, M. Khalilian, 2024. Energy and Exergy Study of a Nanofluid-based Solar System Integrated with a Quadruple Effect Absorption Cycle and Thermoelectric Generator, Iranica Journal of Energy and Environment, 15(1), pp. 80-90. Doi: 10.5829/ijee.2024.15.01.08

$\dot{m}$	Mass flow rate (kg/s)	i	In
n_{cs}	Number of collectors in series	np	Nanoparticle
n_{cp}	Number of collectors in parallels	p	Pump
$\dot{N}$	Outlet flow rate of fluid x (kg/s)	PEM	Proton exchange membrane
P	Pressure (bar)	PTC	Parabolic trough collector
$\dot{Q}$	Heat transfer rate (W)	r	Receiver tube
Q_u	Useful energy gain	TEG	Thermoelectric generator
S	Absorbed solar radiation	th	Thermal
s	Entropy	vg	Vapor generator
T	Temperature (K)	**Greek symbols**	
U_L	Solar collector's overall heat loss coefficient	β	Thickness of the nano-layer relative to the initial radius of the particle
V	Overpotential (V)	η	Efficiency
w	Collector width (m)	$\lambda(x)$	Water content at location x
$\dot{W}$	Net output power (kW)	ρ	Density (kg/m^3)
x	The concentration of refrigerant in the solution	μ	Dynamic viscosity
Z	Investment cost ($)	ϕ	Concentration ratio

INTRODUCTION

Due to the increasing consumption and cost of non-renewable energy such as natural gas and electricity, the utilization of clean and renewable energy like solar energy, geothermal energy, etc. has attracted the attention of researchers in recent years. A significant investigation has been done on the possibility of using solar energy for cooling and heating of different places. Solar energy, as an endless source of energy for the planet, has always occupied a significant part of scientific research. In the last years, the utilization of fossil fuels in the world and Iran has increased dramatically. In addition, an increase in trend of fossil fuel prices and their harmful environmental effects such as pollution, increasing global temperature, and ozone layer destruction has doubled the desire to use renewable and clean energies, such as solar energy. Also, considering that a large part of the energy used up in the summer season is dedicated to the cooling of residential and office buildings and this problem has led to the energy crisis. Therefore, solar chillers can become a suitable substitute for compression chillers, which have high electricity consumption. Absorption refrigeration systems have become famous and popular in recent years from an energy and environmental point of view. Although the absorption chiller has a low coefficient of performance (COP), it can use low-temperature energy such as solar energy, and it also consumes much less electrical energy than the compression cycle, which consumes a great amount of energy due to the presence of a compressor. Another advantage of the solar absorption refrigeration system is the simultaneity of the maximum solar radiation and the maximum cooling load required for air conditioning.

Hydrogen can be generated in different ways such as steam methane reforming, electrolysis, photo-electrocatalysis, and thermolysis. Applying a proton exchange membrane (PEM) water electrolyzer compared with conventional alkaline technology has some benefits like better dynamic operation efficiency, high voltage efficiency at higher current densities, and compact design [1]. Electricity can be generated through direct heat by using thermoelectric generators (TEG). TEGs have no moving part and therefore they work silently. Moreover, they produce no emissions and they have low operating costs [2].

Ketfi et al. [3] investigated the efficiency of a single-effect lithium bromide-water solar absorption refrigeration system with two types of solar collectors: vacuum tube and flat plate collectors. They concluded that to provide 90 kilowatts of input heat to the heat generator, 225.5 square meters are needed if a flat plate collector is used and 175.1 square meters are needed if a vacuum tube collector is used. Tapeh Kaboudy et al. [4] analyzed a single-effect absorption refrigeration cycle connected to solar flat plate and parabolic trough collectors for the city of Kish from an energy and exergy point of view. The results of their research show that the parabolic trough collector compared to the flat plate collector, by absorbing more solar radiation intensity and providing more thermal power in the heat generator, makes it easier to separate the ammonia refrigerant from the water absorber and causes a better performance of the solar absorption refrigeration cycle. Shirazi et al. [5] conducted a parametric study of single, double, and triple-effect solar absorption chillers utilizing common solar collectors in the market. They investigated single-effect absorption chillers with vacuum tube collectors and double-effect, and triple-effect absorption chillers with parabolic trough collectors, Fresnel micro concentrators, and vacuum flat plates. Their results showed that the double-effect absorption chiller combined with the

vacuum flat plate collector performs better both in terms of energy and economy in different climatic conditions. Ozlu and Dincer [6] investigated a multigeneration cycle operated by solar energy. The proposed system produced electricity by using the Kalina cycle and cooling via a four-stage absorption refrigeration cycle. Moreover, hydrogen was produced by applying a PEM electrolyzer. Bellos et al. [7] investigated the efficiency of a single-effect absorption system using four different types of solar collectors. The results of the comparison made it clear that the evacuated tube collector was more economical and the parabolic trough collector led to a higher COP compared with other collectors. Ratlamwala and Abid [8] evaluated the performance of three absorption chillers (single, double, and triple-effect absorption cycles) driven by solar PTC collectors using nanofluid as the working fluid. Results showed that the COP and exergy efficiency of the triple effect chiller was about 31.66% and 16% higher than the double effect cycle, respectively. Bellos et al. [7] studied and compared four different absorption refrigeration cycles using solar energy from the thermodynamic point of view. Nanofluids are applied as the absorbent fluid in the collector. By taking into account different parameters, the outcomes exhibited that applying nanofluids led to higher collector efficiency. Moreover, it was found that the maximum amount of COP and lowest rate of exergy destruction were achieved for the quadruple effect absorption cycle. Abid et al. [9] researched a solar-based absorption refrigeration cycle to provide the cooling effect of a building. The effects of applying magnetic nanoparticles in the collectors and nano refrigerants in the absorption chiller evaporator have been investigated by Rahmani et al. [10]. The results depicted that 250 kJ/h more energy could be absorbed by the solar collectors by just adding 0.5 % nanofluid to the base fluid. Ma et al. [11] investigated a combined solar single/double-effect absorption refrigeration system from thermodynamic and thermoeconomic points of view. The system is designed on a switching method based on the temperature of the solar heat source. The economic results proved that the payback period of the proposed system was 11.84 years. Habibzadeh et al [12] studied the effect of using SiO_2 and TiO_2 nanoparticles on the efficiency of the PTC solar collector in a multigeneration system. The results proved that the solar collector efficiency increases when the nanofluid is applied as the absorbent fluid. Moreover, the highest outlet collector is achieved by using Therminol VP1/SiO_2 nanofluid. Habibollahzade et al. [13] proposed a novel system including a PTC collector, TEG, Rankine cycle, and PEM. In the studied system, the condenser was replaced by TEG to produce more power. According to the results, the rate of hydrogen generated by the system was 2.28 kg/h and the exergy efficiency was achieved to be 13.29%. Finally, it was concluded that using TEG instead of a condenser increases the efficiency of the system and decreases the total cost. Assareh et al. [14] investigated the thermodynamic efficiency of two different renewable energy-based systems to produce hydrogen and electricity. Their system included an ORC cycle, a PEM unit, and TEG. The outcomes presented that when the geothermal system was applied as the heat source, the system produced 11.21% more hydrogen compared with the case solar energy used as the energy source. Musharavati et al. [15] proposed a novel combined cycle containing a solar pond, PEM fuel cell, and TEG. In their study, the TEG was used to recover the waste heat completely. According to the results, the system could generate 2288.8 kW of electricity, and 11.26% and 13.17 % energy and exergy efficiencies were obtained. Gebreslassie et al. [16] investigated on exergy analysis of multieffect water–LiBr absorption systems. Aghagolzadeh Silakhor et al. [17] introduced a Combined Cooling Heating Power (CCHP) system to recover the waste heat of an RK215 heavy diesel engine. The proposed system applied the absorption chiller to produce cooling. For the studied system the energy and exergy efficiencies were 50.46% and 30.8%, respectively.

In summary, the previous studies showed the importance of clean cooling, power, and hydrogen production. To the best knowledge of the authors, although a lot of investigations have been performed on solar-based absorption refrigeration systems, no study investigates the solar collector integration with a quadruple effect absorption refrigeration cycle, TEG unit, and PEM electrolyzer from an energy and exergy point of view. Moreover, the utilization of nanofluids in the solar-based multi-effect absorption refrigeration cycles is rarely studied in the literature. Therefore, in the present study, a solar-assisted quadruple effect absorption refrigeration system for cooling, a TEG as the power generation unit, and a PEM electrolyzer unit for hydrogen production are proposed and analyzed from an energy and exergy point of view. The TEG provides the power needed by the PEM electrolyzer to produce hydrogen. The Al_2O_3/therminol-VP1 nanofluid is utilized in the solar collector as the heat absorbent. Different parameters were studied to find their effects on the performance of the proposed cycle.

SYSTEM DESCRIPTION

Figure 1 depicts the schematic of the nanofluid-based solar-assisted integrated system. The system can be distributed into six parts. The first part is the parabolic trough collector which produces the required energy of the system. The second part is the vapor generator (VG) unit. The third part is the domestic water heater (DWH) to produce the hot water. The fourth part is the quadruple effect (QE) absorption refrigeration cycle to produce cooling. The fifth part is the TEG unit to supply the power needed by the electrolyzer. The sixth part is the PEM electrolyzer which produces hydrogen by water electrolysis. Sunlight irradiates on the parabolic reflector

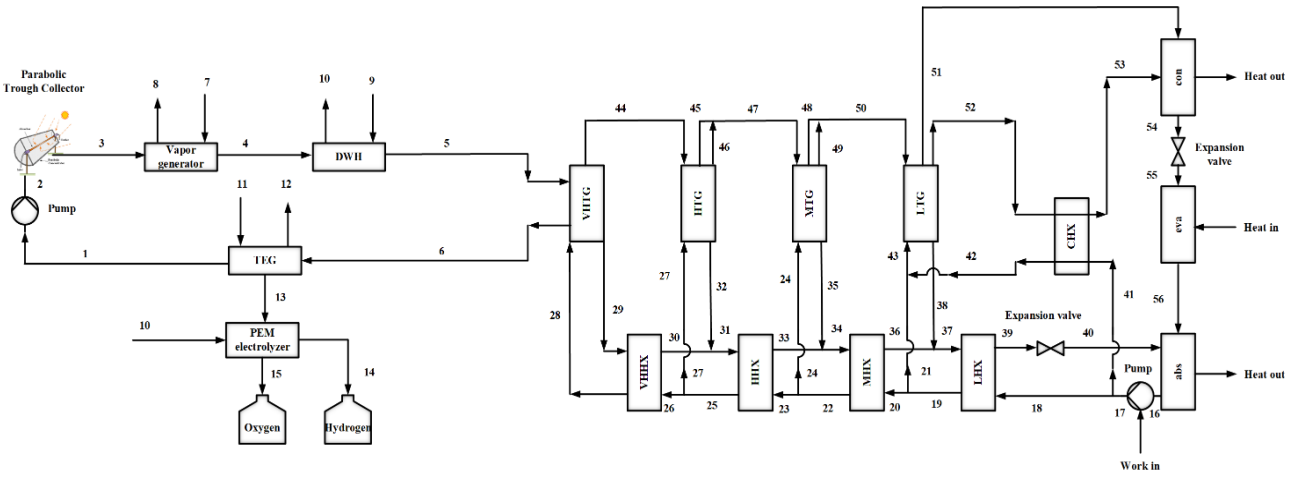

Figure 1. Schematic figure of the nanofluid-based solar multigeneration system

and after reflecting on the absorber, the temperature of the nanofluid in the absorption tube becomes high. The high-temperature nanofluid enters the VG and DWH to present vapor and hot water, respectively. After that, the nanofluid stream enters the VHTG of the QE to generate cooling. Since the nanofluid leaving the absorption refrigeration system is still hot, so the TEG unit is used to recover the remaining excess heat from the nanofluid before entering the solar collector. Finally, the low-temperature nanofluid enters the PTC to reheat.

The working principle of the quadruple effect absorption refrigeration system is as follows: The strong ammonia water solution evacuating the absorber gets into the pump to increase its pressure. Then it is apportioned into two flows. One of the flows enters low, medium, high, and very high-temperature heat exchangers to get heat from the returning stream from the generators and finally, it gets into the VHTG to get heat from the nanofluid to increase the temperature of the strong solution to the boiling point. Boiling leads to the separation of the ammonia from the mixture and then the vapor enters the high, medium, and low-temperature generators to transfer the heat to the strong solution entering the generators. The low-heat ammonia vapor is discharged from the low-temperature generator in two streams: one of the streams directly enters the condenser and the second flow gets into the condenser after proceeding through the heat exchanger of the condenser and giving the heat to the strong solution flows from the pump. In the condenser, the ammonia refrigerant distributes heat to the environment. After moving through the expansion valve, the refrigerant passes into the evaporator to gain heat from the environment. The weak solution flowing from the heat exchangers and ammonia refrigerant is mixed in the absorber and then leave the absorber in the form of a strong solution.

MODELING

In this section, first, the presumptions considered for accomplishing the simulation are presented. Then, the methodologies and governing equations for energy, exergy analysis, as well as the capital investment cost rate of each component, are discussed.

Assumptions

Mathematical modeling and calculation of the integrated system are carried out based on the following assumptions [17]:

- The pipe and heat losses are ignored.
- The system is analyzed based on the steady-state conditions and the ammonia-water solution is considered steady.
- The heat is lost to the environment in the condenser and absorber.
- At the outlet of the condenser, the refrigerant is saturated liquid.
- At the outlet of the evaporator, the refrigerant is saturated vapor.
- At both ends of the expansion valves, the enthalpy is the same.
- Sudden changes in solar radiation have not been assumed in the analysis.

For the thermodynamic investigation of the studied system, the laws of mass conservation and the first and second laws of thermodynamics are used for each component of the proposed cycle. Each component can be used as a control volume for input and output flow, heat transfer, and work interaction [17].

$$\sum \dot{m}_i = \sum \dot{m}_e \quad (1)$$

$$\sum (\dot{m}x)_i = \sum (\dot{m}x)_e \quad (2)$$

$$\sum \dot{m}_i h_i - \sum \dot{m}_e h_e + \sum \dot{Q} - \sum \dot{W} = 0 \quad (3)$$

$$\sum \dot{Q}_k \left(1 - \frac{T_0}{T_k}\right) + \sum \dot{m}_i ex_i = \sum \dot{m}_e ex_e + \sum \dot{W} + \dot{E}x_{D,K} \quad (4)$$

The exergy of fluid flow is defined as follows:

$$ex = [(h_i - h_o) - T_o(s_i - s_o)] \quad (5)$$

Properties of nanofluids

In the present study, the aluminum oxide-Therminol VP1 nanofluid (Al_2O_3-Therminol VP1) is considered as the heat transfer fluid in the collector. The previous studies proved that compared with the base fluids, applying nanofluids results in better thermophysical properties. Table 1 shows the thermodynamic properties of the studied nanoparticle:

To identify the increase in heat transfer through nanofluids, it is necessary to first evaluate the thermophysical properties of nanofluids, such as thermal conductivity, density, viscosity, and specific heat capacity, which must be calculated in the design conditions.

The density of nanofluids (ρ) is presented as follows [18]:

$$\rho_{nf} = \varphi . \rho_{np} + (1 - \varphi) . \rho_{bf} \quad (6)$$

where φ is the nanoparticle volume concentration.

The specific heat capacity of nanofluid (c_p) can be expressed as follows [19]:

$$c_{p,nf} = \frac{\rho_{np} . \varphi . c_{p,np} + \rho_{bf}(1-\varphi) . c_{p,bf}}{\rho_{nf}} \quad (7)$$

The thermal conductivity of nanofluid (k) is calculated using Maxwell's equation as follows [20]:

$$\frac{k_{nf}}{k_{bf}} = \frac{k_{np} + 2k_{bf} + 2(k_{np} - k_{bf}) . (1+\beta)^3 . \varphi}{k_{np} + 2k_{bf} - (k_{np} - k_{bf}) . (1+\beta)^3 . \varphi} \quad (8)$$

In Equation (8), β is defined as the thickness of the nano-layer relative to the initial radius of the particle, and this parameter is usually considered to be 0.1 [21].

The dynamic viscosity of nanoparticle (μ) is estimated by the following relationship [22]:

$$\mu_{nf} = \mu_{bf} . (1 + 2.5\varphi + 6.5\varphi^2) \quad (9)$$

Parabolic trough solar collector

As parabolic collectors have a high acceptance angle, they can absorb both beam and scattered radiation. The nanofluid used as the absorbent fluid passes through the collectors, absorbs the heat of the solar energy, and is directly fed to other subsystems to generate electricity and other outputs. The actual useful energy absorbed in the collector is expressed as follows [23]:

$$Q_u = n_{cp} n_{cs} F_R A_{ap} [S - \frac{A_r}{A_{ap}} U_L (T_{r,i} - T_0)] \quad (10)$$

where n_{cp} and n_{cs} are the number of collectors in parallel and series, respectively. Also, A_{ap} is the collector aperture area, A_r is the receiver area, and F_R is the heat removal factor. In addition, U_L expresses the heat loss coefficient of the entire collector. S shows the absorbed solar radiation and is defined as follows:

$$S = G_b \eta_r \quad (11)$$

$$\eta_r = \gamma \tau_c \tau_p \alpha \quad (12)$$

The areas of the aperture and receiver of the collector are:

$$A_{ap} = (w - D)L \quad (13)$$

$$A_r = \pi D_0 L \quad (14)$$

where $w$is the width, D is the external diameter of the glass cover, and L is the length of the collector.

The following equations can be used to find $F_R$and F_l:

$$F_R = \frac{\dot{m} c_{p,c}}{A_r U_L} [1 - exp(-\frac{A_r U_L F_l}{\dot{m} c_{p,c}})] \quad (15)$$

$$F_1 = \frac{\frac{1}{U_L}}{\frac{1}{U_L} + \frac{D_{r,0}}{h_{fi}} + (\frac{D_{r,0}}{2k} ln \frac{D_{r,0}}{D_{r,i}})} \quad (16)$$

The input heat to the parabolic solar collector is expressed as follows:

$$Q_s = A_{ap} G_b \quad (17)$$

The energy output of the solar collector is determined from the equations proposed by Duffy and Beckman [24] as follows:

$$\eta_{th,PTC} = \frac{Q_u}{Q_s} \quad (18)$$

The input data required for the simulation of the collector is presented in Table 2.

Thermoelectric generator

The energy balance formula for the TEG unit is exhibited as [25]:

$$\dot{Q}_{hot} = \dot{Q}_{cold} + \dot{W}_{TEG} \quad (19)$$

where, $\dot{Q}_{hot}$ and $\dot{Q}_{cold}$ are the TEG's hot and cold side rate of heat transfer and $\dot{W}_{TEG}$ is the amount of the power produced by the TEG unit which can be calculated by:

$$\dot{W}_{TEG} = \eta_{TEG} \times \dot{Q}_{cold} \quad (20)$$

where η_{TEG} is the efficiency of the TEG unit and is defined as [26]:

Table 1. Properties of the studied nanoparticle [22]

Particle	ρ (kg/m^3)	c_p (kJ/kgK)	k (W/mK)
Al_2O_3	3970	0.765	40

Table 2. Input data considered in the simulation of the PTC collector

Parameters	Unit	Value
SOLAR [27, 28]		
Collector width	(m)	5.76
Collector length	(m)	99
Absorber outside diameter	(m)	0.07
Absorber inside diameter	(m)	0.066
Heat loss coefficient of the collector	$(W/m^{2\circ}C)$	3.82
The heat transfer coefficient in the inner side of the receiver	$(W/m^{2\circ}C)$	300
The receiver's thermal conductivity	$(W/m^{2\circ}C)$	16
Solar radiation intensity	$(W/m^{2\circ}C)$	850
Cover glazing transmissivity	-	0.96
Effective transmissivity	-	0.94
Receiver absorptivity	-	0.96
Correction factor for diffuse radiation	-	0.95
Nanoparticle volumetric concentration	(%)	4

$$\eta_{TEG} = \eta_{carnot}\left[\frac{(1+ZT_m)^{0.5}-1}{(1+ZT_m)^{0.5}-\left(\frac{T_{cold}}{T_{hot}}\right)}\right] \quad (21)$$

where, ZT_m is the figure of merit which is between 0.2 to 1.6 depending on the material property [29]. The Carnot efficiency and cold and hot temperatures are presented as:

$$\eta_{carnot} = \left(1-\frac{T_{cold}}{T_{hot}}\right) \quad (22)$$

$$T_{cold} = \frac{1}{2}\left(\frac{T_{11}+T_{12}}{2}\right) \quad (23)$$

$$T_{hot} = \frac{1}{2}\left(\frac{T_6+T_1}{2}\right) \quad (24)$$

The equations required for the modeling of the PEM unit are exhibited in Table 3.

By using fundamental equations for all system types of equipment, the energy, exergy formulas, and cost functions for all types of equipment of the studied system can be determined as described in Tables 4 and 5.

RESULTS AND DISCUSSION

Model validation

After describing all the needed equations to simulate the nanofluid-based parabolic trough collector as well as the other integrated systems, the conclusions of the investigated system are described by using different figures according to the varying parameters. To perform all thermodynamic calculations and especially the thermal properties of the ammonia–H_2O solution, EES software [33] was applied. To validate the absorption system investigated in the present study, the cycle proposed by Ratlamwala and Abid [8] is applied. The exergetic COP of the triple effect absorption system is validated for the case the evaporator temperature is assumed to be 13℃. The temperature of the generator varies between 127 to 177 ℃. The comparative analysis is shown in Figure 2 which shows a reasonable agreement.

Table 3. Equations required for the modeling of the PEM unit

PEM [30]	
Electrical energy consumption	$\dot{E}_{electric} = JV$
Electrolyzer voltage	$V = V_0 + V_{act,c} + V_{act,a} + V_{ohm}$
Reversible equation	$V_0 = 1.229 - 0.00085(T_{PEM} - 298)$
Activation overpotential	$J_a^{ref}\ exp\left(\frac{-E_{act,i}}{RT}\right), i = a, c$
Ohmic overpotential	$V_{ohm} = JR_{PEM}, R_{PEM} = \int_0^L \frac{dx}{\sigma[\lambda(x)]}, \lambda(x) = \frac{\lambda_a-\lambda_c}{D}x + \lambda_c\ \sigma[\lambda(x)] = [0.5139\lambda(x) - 0.326]\ exp\left[1268\left(\frac{1}{303}-\frac{1}{T}\right)\right]$
Rate of produced H_2	$\dot{N}_{H_2,Out} = \frac{J}{2F} = \dot{N}_{H_2O,reacted}$

Table 4. The cost functions applied for the different parts of the studied system

Components	The cost functions [31, 32]
PTC	$Z_{PTC} = 240 \times A_a$
Absorption chiller	$Z_{ARS} = 1144.3 \times (\dot{Q}_{eva})^{0.67}$
Vapor generator	$Z_{vg} = 1397 \times (A_{vg})^{0.89}$
PEM	$Z_{PEM} = 1000 \times \dot{W}_{pem}$
DWH	$Z_{DWH} = 130 \times (\frac{A_{DWH}}{0.093})^{0.78}$
TEG	$Z_{TEG} = 1500 \times \dot{W}_{TEG}$

Results of parametric study

Table 6 depicts the overall performance of the proposed system under the basic defined conditions.

One of the factors that affect the increase in useful energy produced by the solar collector is the volume percentage of nanoparticles. Figure 3 shows the changes in useful energy obtained and power produced by the TEG unit against the percentage of Al_2O_3 nanoparticles. It is inferred that an increase in the percentage of nanoparticles leads to an increase in the useful energy obtained from the PTC collector. According to defined equations, changing the concentration of nanoparticles only changes the coefficient of heat transfer. By

Table 5. Energy and exergy equation of the proposed system

Components	Energy equations	Exergy equations
PTC	$\dot{m}_2 h_2 + \dot{Q}_u = \dot{m}_3 h_3$	$\dot{E}x_{D,PTC} = \dot{E}x_{sun} + \dot{E}x_2 - \dot{E}x_3$
Vapor generator	$\dot{Q}_{vg} = \dot{m}_3(h_3 - h_4) = \dot{m}_7(h_8 - h_7)$	$\dot{E}x_{D,vg} = \dot{E}x_3 + \dot{E}x_7 - \dot{E}x_4 - \dot{E}x_8$
DWH	$\dot{Q}_{DWH} = \dot{m}_4(h_4 - h_5) = \dot{m}_9(h_{10} - h_9)$	$\dot{E}x_{DWH} = \dot{E}x_4 + \dot{E}x_9 - \dot{E}x_5 - \dot{E}x_{10}$
TEG	$\dot{Q}_{TEG} = \dot{m}_6(h_6 - h_1) = \dot{m}_{11}(h_{12} - h_{11})$	$\dot{E}x_{TEG} = \dot{E}x_6 + \dot{E}x_{11} - \dot{E}x_1 - \dot{E}x_{12}$
PEM	$\dot{W}_{PEM} = (\dot{m}_{10}h_{10} - \dot{m}_{14}h_{14} - \dot{m}_{15}h_{15})$	$\dot{E}x_{D,PEM} = \dot{E}x_{10} + \dot{W}_{PEM} - \dot{E}x_{14} - \dot{E}x_{15}$
ARC absorber	$\dot{Q}_{abs,ARS} = \dot{m}_{56}h_{56} + \dot{m}_{40}h_{40} - \dot{m}_{16}h_{16}$	$\dot{E}x_{D,abs,ARS} = \dot{E}x_{11} + \dot{E}x_{16} - \dot{E}x_1 - \left(1 - \frac{T_0}{T_{16}}\right)\dot{Q}_{abs}$
ARC condenser	$\dot{Q}_{con,ARS} = \dot{m}_{51}h_{51} + \dot{m}_{53}h_{53} - \dot{m}_{54}h_{54}$	$\dot{E}x_{D,con,ARS} = \dot{E}x_{51} + \dot{E}x_{53} - \dot{E}x_{54} - \left(1 - \frac{T_0}{T_{54}}\right)\dot{Q}_{con}$
ARC evaporator	$\dot{Q}_{eva,ARS} = \dot{m}_{55}(h_{56} - h_{55})$	$\dot{E}x_{D,eva,ARS} = \dot{E}x_{10} - \dot{E}x_{11} + \left(1 - \frac{T_0}{T_{56}}\right)\dot{Q}_{eva}$
ARC VHTG	$\dot{Q}_{VHTG,ARS} = \dot{m}_{29}h_{29} + \dot{m}_{44}h_{44} - \dot{m}_{28}h_{28}$	$\dot{E}x_{D,VHTG,ARS} = \dot{E}x_{28} - \dot{E}x_{29} - \dot{E}x_{44} + \left(1 - \frac{T_0}{T_{44}}\right)\dot{Q}_{VHTG}$
ARC HTG	$\dot{Q}_{HTG,ARS} = \dot{m}_{44}h_{44} - \dot{m}_{45}h_{45}$	$\dot{E}x_{D,HTG,ARS} = \dot{E}x_{27} - \dot{E}x_{32} - \dot{E}x_{46} - \left(1 - \frac{T_0}{T_{32}}\right)\dot{Q}_{HTG}$
ARC MTG	$\dot{Q}_{MTG,ARS} = \dot{m}_{47}h_{47} - \dot{m}_{48}h_{48}$	$\dot{E}x_{D,MTG,ARS} = \dot{E}x_{24} - \dot{E}x_{35} - \dot{E}x_{49} - \left(1 - \frac{T_0}{T_{35}}\right)\dot{Q}_{MTG}$
ARC LTG	$\dot{Q}_{LTG,ARS} = \dot{m}_{50}h_{50} - \dot{m}_{51}h_{51}$	$\dot{E}x_{D,LTG,ARS} = \dot{E}x_{43} - \dot{E}x_{52} - \dot{E}x_{38} - \left(1 - \frac{T_0}{T_{38}}\right)\dot{Q}_{LTG}$
ARC Pump	$\dot{W}_{p,ARS} = \dot{m}_{16}(h_{17} - h_{16})$	$\dot{E}x_{D,p,ARS} = \dot{E}x_{16} + \dot{W}_p - \dot{E}x_{17}$
COP	$COP_{en} = \frac{\dot{Q}_{eva}}{\dot{Q}_{VHTG} + \dot{W}_p}$	$COP_{ex} = \frac{\dot{E}x_{th,eva}}{\dot{E}x_{th,VHTG} + \dot{W}_p}$

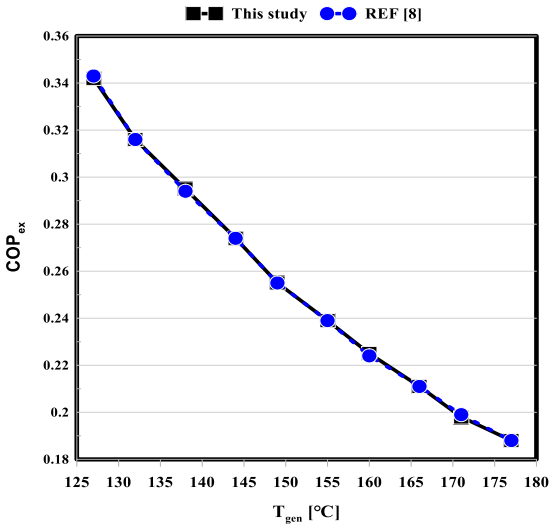

Figure 2. A comparison of the exergetic COP of the triple effect absorption refrigeration system based on literature [8]

increasing the concentration of nanoparticles, the mass flow rate of nanofluid increases while the specific heat transfer decreases. By changing the ratio from 0 to 0.06, the useful energy increases from 9965 to 10376 kW. On the other hand, when the nanoparticle concentration goes up, the amount of generated power in the TEG unit decreases. By raising the percentage of nanoparticles, the exit temperature of the collector reduces which causes a reduction in the amount of TEG efficiency. Reduction in the amount of TEG efficiency causes a decrease in the amount of power generated in the TEG unit.

Figure 4 demonstrates the tendency of useful energy obtained by PTC and hydrogen production rate when the

Table 6. The main results of the proposed multigeneration system

Parameters	Results
$\eta_{en,PTC}(\%)$	82.21
$\eta_{ex,PTC}(\%)$	80.48
$Q_u(kW)$	10240
$\dot{Q}_{VG}(kW)$	161.3
$\dot{Q}_{DWH}(kW)$	30.07
$\dot{Q}_{cooling}(kW)$	445.7
$\dot{W}_{TEG}(kW)$	18.78
COP_{en}	1.527
COP_{ex}	0.936
$\dot{m}_{H2}(g/s)$	0.000742
$Z(\$)$	69055

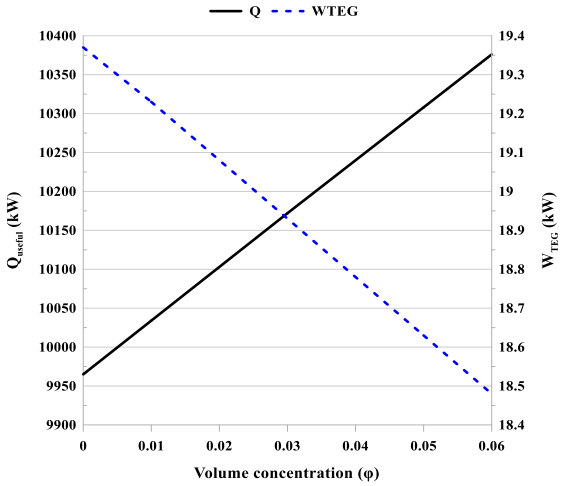

Figure 3. The effect of volume concentration of nanoparticles on the useful energy obtained from the collector and generated power in the TEG unit

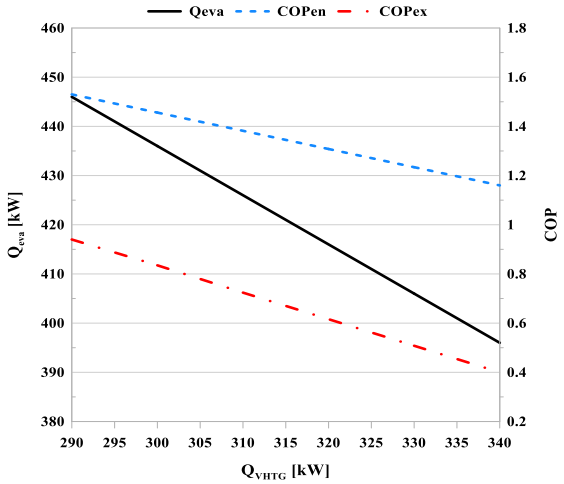

Figure 5. The effect of VHTG load on the cooling content and COPs of the absorption refrigeration system

amount of solar radiation changes from 400 to 850 W/m^2 and the percentage of nanoparticles is fixed at 0.04. When the amount of solar radiation increases, the amount of power generated by the TEG is decreased, which decreases the rate of hydrogen produced. In addition, the absorbed solar radiation increases with the rise in the solar radiation which causes an increase in the useful energy obtained by the collector. As the solar radiation changes from 400 to 850 W/m^2, the amount of useful energy obtained by Al_2O_3-based nanofluid changes from 4813 to 10240 kW.

Figure 5 exhibits the effect of alternation in the very high-temperature generator load on the cooling content and energy and exergy COPs of the quadruple effect absorption refrigeration system. It is observed that by increasing the VHTG load from 290 to 340 kW, the rate of cooling generated by the system decreases from 446.2 to 396.3 kW. The main reason for the decrease in the cooling capacity is that increase in VHTG capacity leads to a higher outlet ammonia vapor temperature which enters the evaporator. Lower cooling capacity is produced when there is a small temperature distribution between the evaporator inlet and outlet. Moreover, the energy and exergy COPs are decreased by rising VHTG load. The reduction in the cooling load with the rise in the VHTG capacity, negatively influences the efficiency of the system and for that, both COPs are reduced.

The variation of the concentration of the strong solution on the amount of produced cooling and energy and exergy COPs are exhibited in Figure 6. One of the main factors which considerably affects the performance of refrigeration systems is the concentration of the strong

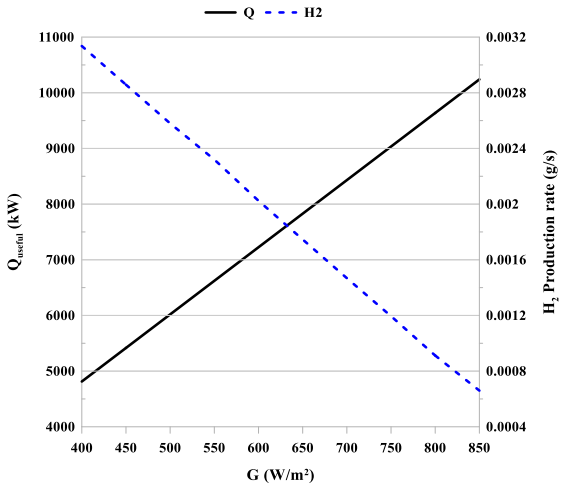

Figure 4. The effect of solar radiation on the useful energy obtained from the collector and the hydrogen production rate of the system

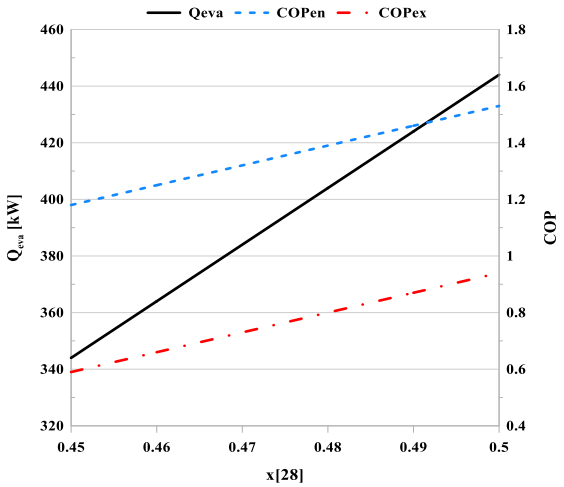

Figure 6. The effect of the concentration of the strong solution on the cooling content and COPs of the absorption refrigeration system

solution which is the amount of the refrigerant vaporizes and enters the evaporator. By increasing the concentration of the strong solution, the rate of produced cooling changes from 342.1 to 443.2 kW. A higher quantity of ammonia is vaporized from VHTG when an increase in the strong solution concentration happens and eventuates in the production of more cooling capacity in the evaporator. On the other hand, energy and exergy COPs of the refrigeration system tend to have an increasing trend by increasing solution concentration. It should be noted that the COPs of the system are straightly relevant to the cooling generation load of the system.

The figure of merit (ZT) is a dimensionless parameter that is used to show the performance and efficiency of the TEG and a higher amount of ZT proves better performance of TEG. The variation of TEG performance and output power with the figure of merit is depicted in Figure 7. According to the graphs, it can be inferred that rising ZT leads to an increase in the amounts of TEG efficiency and generated power. It can be observed that with an increment in ZT from 0.2 to 2, the value of the generated power in TEG changes from 104.4 to 216 kW while the efficiency of TEG varies between 0.56 to 1.17%.

Figure 8 shows the relative amounts of exergy destruction rate for the subsystems of the proposed multigeneration cycle. The figure depicts that solar collector has the highest amount of exergy destruction rate which is 4461 kW. The main reason for the higher exergy destruction rate in the solar collector is the higher rate of the PTC's heat loss. The second and third highest exergy destruction rates happen in the absorption refrigeration system and vapor generator, respectively. Moreover, it can be inferred that the lowest exergy destruction rate among different subsystems refers to the domestic water heater.

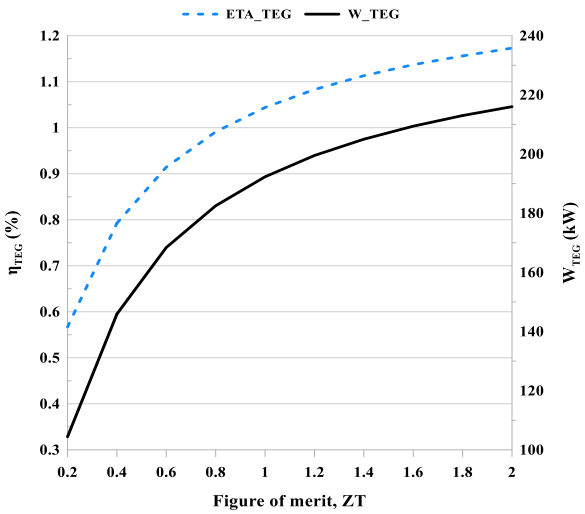

Figure 7. Effects of ZT on the efficiency and produced power of TEG unit

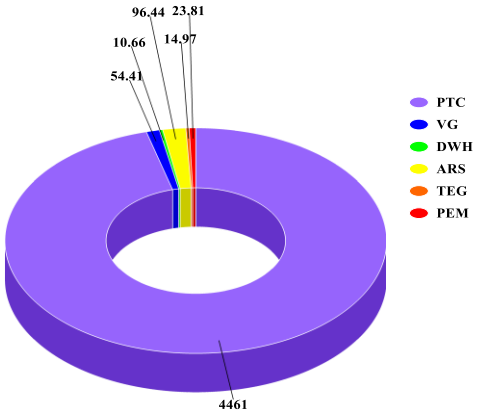

Figure 8. The share of each subsystem to the total amount of exergy destruction

CONCLUSION

Solar energy conversion systems using nanofluids as the working fluid in solar thermal systems solve the problem of low thermal performance of these systems. This is considered an innovative approach to ameliorate thermal performance and make the systems more stable. The present investigations deal with the energy and exergy analysis of a multigeneration system in which solar energy is used as the energy source to meet the needs of the combined cycle. The proposed system can produce cooling, power, hydrogen, vapor, and hot water. Aluminum oxide is used as nanoparticles in the therminol VP1 as the base fluid in the solar collector. Several parameters such as the volume concentration of nanoparticles, the intensity of solar radiation, VHTG load, the concentration of the strong solution, and the figure of merit of the TEG unit were investigated separately to evaluate their efficacy on the overall system. System modeling was done by the EES program under the specified conditions. The summary of the main outcomes can be described:

- The total energy and exergy efficiency of the solar collector using Al_2O_3-Therminol VP1 nanofluid fluid was 82.21% and 80.48%, respectively.
- The highest amount of exergy destruction in overall systems occurred in the solar system which is followed by the absorption refrigeration system and vapor generator. Therefore, the overall exergy performance of the multigeneration system can be improved by modifying the components with higher exergy degradation rates.
- The results showed that by increasing the percentage of nanoparticles and solar irradiation, the useful energy obtained from the collector is increased while the power generated by the TEG unit and the hydrogen production rate is decreasing.
- When the HTVG load changes from 290 to 340 kW, the cooling generated by the system and the COPs of the absorption system decrease.

- ❖ Increasing the concentration of the strong solution has a positive effect on the system performance and increases the cooling load and COPs of the studied system.
- ❖ The power produced by the TEG unit and the efficiency of the TEG unit has an upward trend when the figure of merit rises.

REFERENCES

1. Ahmadi, P., Dincer, I., and Rosen, M.A., 2013. Energy and exergy analyses of hydrogen production via solar-boosted ocean thermal energy conversion and PEM electrolysis. *International Journal of Hydrogen Energy*, 38(4), pp.1795–1805. Doi: 10.1016/j.ijhydene.2012.11.025
2. Demir, M.E., and Dincer, I., 2017. Development of a hybrid solar thermal system with TEG and PEM electrolyzer for hydrogen and power production. *International Journal of Hydrogen Energy*, 42(51), pp.30044–30056. Doi: 10.1016/j.ijhydene.2017.09.001
3. Ketfi, O., Merzouk, M., Merzouk, N.K., and Metenani, S. El, 2015. Performance of a Single Effect Solar Absorption Cooling System (Libr-H2O). *Energy Procedia*, 74, pp.130–138. Doi: 10.1016/j.egypro.2015.07.534
4. Tapeh Kaboudy, R., Suori, E. and Seyed Shams Taleghani S.A., 2016. "Investigation of thermodynamic analysis and exergy of a single effect solar absorption refrigeration cycle with parabolic collectors and the agent fluid of water and ammonia", 1st International Conference on Mechanical Engineering and Aerospace, University of Tehran, Tehran, Iran. [In Persian]
5. Shirazi, A., Taylor, R.A., White, S.D., and Morrison, G.L., 2016. A systematic parametric study and feasibility assessment of solar-assisted single-effect, double-effect, and triple-effect absorption chillers for heating and cooling applications. *Energy Conversion and Management*, 114, pp.258–277. Doi: 10.1016/j.enconman.2016.01.070
6. Ozlu, S., and Dincer, I., 2015. Development and analysis of a solar and wind energy based multigeneration system. *Solar Energy*, 122, pp.1279–1295. Doi: 10.1016/j.solener.2015.10.035
7. Bellos, E., Tzivanidis, C., and Antonopoulos, K.A., 2016. Exergetic, energetic and financial evaluation of a solar driven absorption cooling system with various collector types. *Applied Thermal Engineering*, 102, pp.749–759. Doi: 10.1016/j.applthermaleng.2016.04.032
8. Ratlamwala, T.A.H., and Abid, M., 2018. Performance analysis of solar assisted multi-effect absorption cooling systems using nanofluids: A comparative analysis. *International Journal of Energy Research*, 42(9), pp.2901–2915. Doi: 10.1002/er.3980
9. Abid, M., Khan, M.S., Ratlamwala, T.A.H., Malik, M.N., Ali, H.M., and Cheok, Q., 2021. Thermodynamic analysis and comparison of different absorption cycles driven by evacuated tube solar collector utilizing hybrid nanofluids. *Energy Conversion and Management*, 246, pp.114673. Doi: 10.1016/j.enconman.2021.114673
10. Rahmani, M., Shahabi Nejad, A., Fallah Barzoki, M., Kasaeian, A., and Sameti, M., 2022. Simulation of solar absorption refrigeration cycle with CuO nanofluid for summer cooling of a residential building. *Thermal Science and Engineering Progress*, 34, pp.101419. Doi: 10.1016/j.tsep.2022.101419
11. Ma, H., Li, Q., Wang, D., Song, Q., Zhou, S., Wang, X., and Li, Y., 2022. Operating performance and economic analysis of solar single/double-effect compound absorption refrigeration system. *Solar Energy*, 247, pp.73–85. Doi: 10.1016/j.solener.2022.10.005
12. Habibzadeh, A., Abbasalizadeh, M., Mirzaee, I., Jafarmadar, S., and Shirvani, H., 2023. Thermodynamic Modeling and Analysis of a Solar and Geothermal-driven Multigeneration System Using TiO2 and SiO2 Nanoparticles. *Iranian Journal of Energy and Environment*, 14(2), pp.127–138. Doi: 10.5829/IJEE.2023.14.02.05
13. Habibollahzade, A., Gholamian, E., Ahmadi, P., and Behzadi, A., 2018. Multi-criteria optimization of an integrated energy system with thermoelectric generator, parabolic trough solar collector and electrolysis for hydrogen production. *International Journal of Hydrogen Energy*, 43(31), pp.14140–14157. Doi: 10.1016/j.ijhydene.2018.05.143
14. Assareh, E., Delpisheh, M., Farhadi, E., Peng, W., and Moghadasi, H., 2022. Optimization of geothermal- and solar-driven clean electricity and hydrogen production multi-generation systems to address the energy nexus. *Energy Nexus*, 5, pp.100043. Doi: 10.1016/j.nexus.2022.100043
15. Musharavati, F., Khanmohammadi, S., Nondy, J., and Gogoi, T.K., 2022. Proposal of a new low-temperature thermodynamic cycle: 3E analysis and optimization of a solar pond integrated with fuel cell and thermoelectric generator. *Journal of Cleaner Production*, 331, pp.129908. Doi: 10.1016/j.jclepro.2021.129908
16. Gebreslassie, B.H., Medrano, M., and Boer, D., 2010. Exergy analysis of multi-effect water–LiBr absorption systems: From half to triple effect. *Renewable Energy*, 35(8), pp.1773–1782. Doi: 10.1016/j.renene.2010.01.009
17. Aghagolzadeh Silakhor, R., Jahanian, O., and Alizadeh Kharkeshi, B., 2023. Investigating a Combined Cooling, Heating and Power System from Energy and Exergy Point of View with RK-215 ICE Engine as a Prime Mover. *Iranica Journal of Energy and Environment*, 14(1), pp.65–75. Doi: 10.5829/IJEE.2023.14.01.09
18. Duangthongsuk, W., and Wongwises, S., 2010. An experimental study on the heat transfer performance and pressure drop of TiO2-water nanofluids flowing under a turbulent flow regime. *International Journal of Heat and Mass Transfer*, 53(1–3), pp.334–344. Doi: 10.1016/j.ijheatmasstransfer.2009.09.024
19. Ghasemi, S.E., and Ranjbar, A.A., 2016. Thermal performance analysis of solar parabolic trough collector using nanofluid as working fluid: A CFD modelling study. *Journal of Molecular Liquids*, 222, pp.159–166. Doi: 10.1016/j.molliq.2016.06.091
20. Kasaeian, A.B., 2012. Convection Heat Transfer Modeling of Ag Nanofluid Using Different Viscosity Theories. *IIUM Engineering Journal*, 13(1). Doi: 10.31436/iiumej.v13i1.149
21. Khanafer, K., and Vafai, K., 2011. A critical synthesis of thermophysical characteristics of nanofluids. *International Journal of Heat and Mass Transfer*, 54(19–20), pp.4410–4428. Doi: 10.1016/j.ijheatmasstransfer.2011.04.048
22. Borgnakke, C. and Sonntag, R.E., 2020. Fundamentals of thermodynamics. John Wiley & Sons.
23. Yu, W., and Choi, S.U.S., 2003. The Role of Interfacial Layers in the Enhanced Thermal Conductivity of Nanofluids: A Renovated Maxwell Model. *Journal of Nanoparticle Research*, 5(1/2), pp.167–171. Doi: 10.1023/A:1024438603801
24. Duffie, J.A. and Beckman, W.A., 2013. Solar engineering of thermal processes. John Wiley & Sons.
25. Malik, M.Z., Musharavati, F., Khanmohammadi, S., Baseri, M.M., Ahmadi, P., and Nguyen, D.D., 2020. Ocean thermal energy conversion (OTEC) system boosted with solar energy and TEG based on exergy and exergo-environment analysis and multi-objective optimization. *Solar Energy*, 208, pp.559–572. Doi: 10.1016/j.solener.2020.07.049
26. Aliahmadi, M., Moosavi, A., and Sadrhosseini, H., 2021. Multi-objective optimization of regenerative ORC system integrated with thermoelectric generators for low-temperature waste heat recovery. *Energy Reports*, 7, pp.300–313. Doi: 10.1016/j.egyr.2020.12.035
27. Kalogirou, S.A., 2013. Solar energy engineering: processes and systems. Academic press.

28. Keshtkar, M.M., and Khani, A.G., 2018. Exergoeconomic analysis and optimization of a hybrid system based on multi-objective generation system in Iran: a case study. *Renewable Energy Focus*, 27, pp.1–13. Doi: 10.1016/j.ref.2018.07.008
29. Chávez-Urbiola, E.A., Vorobiev, Y.V., and Bulat, L.P., 2012. Solar hybrid systems with thermoelectric generators. *Solar Energy*, 86(1), pp.369–378. Doi: 10.1016/j.solener.2011.10.020
30. M., A., S., K., and S., J., 2019. Energy and Exergy Analysis of a New Power, Heating, Oxygen and Hydrogen Cogeneration Cycle Based on the Sabalan Geothermal Wells. *International Journal of Engineering, Transactions C: Aspects*, 32(3), pp.445–450. Doi: 10.5829/ije.2019.32.03c.13
31. Yu, Z., Su, R., and Feng, C., 2020. Thermodynamic analysis and multi-objective optimization of a novel power generation system driven by geothermal energy. *Energy*, 199, pp.117381. Doi: 10.1016/j.energy.2020.117381
32. Ahmadi, P., Dincer, I., and Rosen, M.A., 2014. Multi-objective optimization of a novel solar-based multigeneration energy system. *Solar Energy*, 108, pp.576–591. Doi: 10.1016/j.solener.2014.07.022
33. Klein, S.A. and Alvarado, F.L., 2011. Engineering Equation Solver (EES), FChart Software.

Persian Abstract

چکیده

بهره‌برداری از نانوسیال‌ها قابل توجه‌ترین راه برای بهتر کردن سرعت انتقال حرارت کلکتورهای خورشیدی می‌باشد. علاوه بر این، اخیراً استفاده از ژنراتورهای ترموالکتریک به طور گسترده برای تبدیل مستقیم گرما به الکتریسیته مورد مطالعه قرار گرفته است. هدف از این تحقیق مطالعه یک سیستم جدید تولید چندگانه است که شامل یک کلکتور سهموی مبتنی بر نانوسیال ترکیب شده با یک سیستم تبرید چهار اثره (برای تولید سرمایش)، یک ژنراتور ترموالکتریک (برای تولید توان)، یک الکترولایزر با غشای تبادل پروتون (برای تولید هیدروژن)، مولد بخار و آبگرمکن خانگی می‌باشد. یک مطالعه پارامتری برای در نظر گرفتن تأثیر پارامترهای مهم مانند غلظت حجمی نانوذرات، تابش خورشیدی، بار مولد سیستم جذبی و غلظت محلول قوی و رقم شایستگی ژنراتور ترموالکتریک بر عملکرد کلی سیستم، نرخ تولید هیدروژن، بار سرمایشی، ضریب عملکرد و انرژی مفید بدست آمده توسط کلکتور انجام شده است. از نتایج شبیه‌سازی مشاهده می‌شود که توان تولید شده توسط سیستم در شرایط پایه تعریف شده ۱۸/۷۸ کیلو وات و بازده انرژی و اگزرژی کلکتور به ترتیب ۸۲/۲۱٪ و ۸۰/۴۸٪ می‌باشد. علاوه بر این، نتایج نشان داد که بیشترین میزان تخریب اگزرژی در سیستم خورشیدی با نرخ ۴۴۶۱ کیلووات رخ می‌دهد. ضریب عملکردهای انرژی و اگزرژی سیستم جذبی به ترتیب ۱/۵۲۷ و ۰/۹۳۶ است. با افزایش غلظت نانوذرات و میزان تابش خورشید، مقدار انرژی مفید کلکتور افزایش می‌یابد در حالی که میزان تولید هیدروژن و توان تولیدی در ژنراتور ترموالکتریک کاهش می‌یابد. بار سرمایشی و ضریب‌های عملکردی سیستم جذبی با افزایش بار ژنراتور با دمای بسیار بالا افزایش می‌یابد و با افزایش غلظت محلول قوی کاهش می‌یابد.